

# The Extension Method for Bloch Branes

F. A. Brito<sup>a,b\*</sup>, L. Losano<sup>b†</sup> and J. R. L. Santos<sup>a‡</sup>

<sup>a</sup>*Unidade Acadêmica de Física,  
Universidade Federal de Campina Grande,  
58429-900 Campina Grande, Paraíba, Brazil*

<sup>b</sup>*Departamento de Física,  
Universidade Federal da Paraíba,  
58051-900 João Pessoa, Paraíba, Brazil*

The present work unveils a new procedure to determine analytical hybrid braneworld models. The discussions were based on the so-called Block branes, which are constructed via a two-field model coupled with gravity in 5-dimensional spacetime. Both fields used to build the Block branes depend only on the extra dimension and such branes are considered thick, once they have internal structure. In this work, we were able to derive new analytical thick brane models by using an extension method. Some of these new branes unveil a Minkowski space-time immersed inside of the fifth-dimension. We showed how the symmetry of the emergent branes can be controlled via specific parameters. We also analyzed the stability conditions for each derived model.

PACS numbers: 11.25.-w, 05.45.Yv, 03.65.Vf, 11.27.+d

## I. INTRODUCTION

In their seminal papers, Randall and Sundrum [1, 2] proposed a new route to possibly solve the hierarchy problem by using a new set of metric with an extra dimension. This metric has the property of being non-factorizable, where the standard four-dimensional metric is multiplied by a warp factor which grows exponentially as a function of the compactification radius. The so-called Randall-Sundrum braneworld model gave rise to a thin brane profile which contains the Standard Model of fields, and it is an effective mechanism to reduce the energy scales from Planckian to TeV. Nevertheless, the search for models with thick branes has grown in the last decade, since the seminal work of Arkani-Hamed and Schmaltz [3], where the authors showed that the expectation for the stability of the proton as being originated from high-energy theories, could be violated if the Standard Model is confined into a thick wall.

Several different argumentations for generating models with thick branes have been proposed in the literature, and most of them include the coupling of gravity with a scalar field, where the last depends only on the extra-dimension. One of this approaches is the so-called Block branes, introduced by Bazeia and Gomes [4] where the authors inspired themselves in a condensed matter model denominated Block walls (these are domain walls with internal structure), in the context of braneworlds scenarios. These branes are hybrid ones, which means that they are generated by multiscalar fields models (in this case, a two scalar fields model). There the authors were able to find analytical warp factor, as well as to verify the localization of gravity, by computing the graviton zero-mode. One feature related with the branes of such a model is that they are symmetric, and as it was pointed by [5, 6] a certain degree of asymmetry for the brane is desired in order to have models which are useful to deal with the hierarchy problem. In this work, we propose to generalize the initial Bloch branes approach by generating new exactly solvable braneworld models via an extension method introduced in [7].

In our investigation, we are going to use some parameters to control the asymmetry of the brane. Moreover, we are going to verify carefully the stability of such branes, besides we compute the zero-mode states for each new braneworld family. The set of ideas behind our investigation is divided into the following sections: In section II we describe some generalities about hybrid branes models. In section III we show the main ingredients necessary to implement the extension method. In section IV we apply the extension method in the braneworld scenario, and we exemplify it with three cases called  $\phi^4$  versus  $\chi^6$ ,  $p$  versus  $p$ , and  $\phi^4$  versus  $p$ . Section V is dedicated to verifying the stability of each braneworld model derived in the previous section. Finally, we left our perspectives and final discussions for section VI.

---

\* email: fabrito@df.ufcg.edu.br

† email: losano@fisica.ufpb.br

‡ email: joaorafael@df.ufcg.edu.br

## II. GENERALITIES

In this section, we present some generalities concerning the application of scalar fields in braneworld scenarios, by following the recipe adopted in [4]. Here, we studied the coupling between a two scalar field Lagrangian with gravity in  $4 + 1$  dimensions, which means that in this representation the spacetime has an extra spatial coordinate named  $y$ . So, the action related to this previous Lagrangian is such that

$$S = \int d^4x dy \sqrt{|g|} \left[ -\frac{R}{4} + \mathcal{L}(\phi, \partial_a \phi; \chi, \partial_a \chi) \right], \quad (1)$$

where we consider the standard form for  $\mathcal{L}$ , which means

$$\mathcal{L} = \frac{1}{2} \partial_a \phi \partial^a \phi + \frac{1}{2} \partial_a \chi \partial^a \chi - V(\phi, \chi). \quad (2)$$

In this approach we are working with  $4\pi G = 1$ ,  $g$  is the determinant of the metric tensor  $g_{ab}$ , and the square of the line element is

$$ds_5^2 = g_{ab} dx^a dy^b = e^{2A(y)} \eta_{\mu\nu} dx^\mu dx^\nu - dy^2, \quad (3)$$

with  $a, b = 0, 1, \dots, 4$ ,  $\nu, \mu = 0, 1, \dots, 3$ ,  $\eta_{\mu\nu} = (1, -1, -1, -1)$ , besides  $e^{2A}$  is the so-called warp-factor. In order to find a stable brane, the warp-factor needs to be integrable, which means that

$$\lim_{y \rightarrow \pm\infty} e^{2A(y)} = 0. \quad (4)$$

Moreover, from Eq. (3) we yield to the 4D Minkowski spacetime by taking  $y = 0$ , and for the asymptotic values of  $y$ , we have  $ds^2 = -dy^2$ , which means a space-like interval in the fifth dimension. The Einstein's equations for such a configuration are given by

$$G_{ab} = 2T_{ab}, \quad (5)$$

where  $T_{ab}$  is the energy momentum tensor in  $4 + 1$  dimensions. If we deal with  $\phi = \phi(y)$ ,  $\chi = \chi(y)$ , and  $A = A(y)$ , we can derive the following equations of motion for a braneworld model

$$\phi'' + 4A'\phi' = V_\phi; \quad \chi'' + 4A'\chi' = V_\chi, \quad (6)$$

besides, once we are working with flat branes, the parameter  $A$  must satisfy the equations

$$A'' = -\frac{2}{3} (\phi'^2 + \chi'^2), \quad (7)$$

and

$$A'^2 = \frac{1}{6} (\phi'^2 + \chi'^2) - \frac{1}{3} V, \quad (8)$$

where primes mean derivatives in respect to  $y$ . In order to implement the first-order formalism, let us establish the definitions

$$A' = -\frac{W}{3}; \quad \phi' = \frac{W_\phi}{2}; \quad \chi' = \frac{W_\chi}{2}, \quad (9)$$

where  $W = W(\phi, \chi)$ . Thus, the potential  $V$  needs to obey the constraint

$$V(\phi, \chi) = \frac{1}{8} (W_\phi^2 + W_\chi^2) - \frac{W^2}{3}, \quad (10)$$

furthermore, the energy density for this system is described by

$$\rho(y) = e^{2A(y)} \left[ \frac{\phi'^2}{2} + \frac{\chi'^2}{2} + V(\phi, \chi) \right]. \quad (11)$$

So, once we solve the first-order differential equations for  $\phi$  and  $\chi$ , we can determine an analytical warp-factor. However, the main difficulty concerning analytical results for two field models is that in general, these first-order differential equations are coupled, which make them hard to be integrated.

### III. EXTENSION METHOD

With the purpose to determine new analytical effective two scalar fields models in braneworld scenarios, we are going to use the extension method presented by [7]. In order to apply such a method, let us verify that the last two equations of (9) can be rearranged as

$$\phi_\chi = \frac{\phi'}{\chi'} = \frac{W_\phi(\phi, \chi)}{W_\chi(\phi, \chi)}, \quad (12)$$

whose integration lead us to analytical orbits relating  $\phi$  and  $\chi$ . Before we discuss the generalities about the extension procedure, we may describe some main points related to the so-called deformation method introduced by [12].

Given the two standard classical field theory Lagrangians

$$\mathcal{L} = \frac{1}{2} \partial_\mu \phi \partial^\mu \phi - V(\phi); \quad \mathcal{L}_d = \frac{1}{2} \partial_\mu \chi \partial^\mu \chi - \tilde{V}(\chi), \quad (13)$$

where the real fields  $\phi$  and  $\chi$  are statical, one dimensional, and need to obey the equations of motion

$$-\phi'' + V_\phi = 0; \quad -\chi'' + \tilde{V}_\chi = 0, \quad (14)$$

then, by applying the BPS method, the solutions of these second-order differential equations may satisfy

$$\phi' = W_\phi(\phi); \quad \chi' = W_\chi(\chi), \quad (15)$$

where we assumed that  $V$  and  $\tilde{V}$  are defined as

$$V = \frac{W_\phi^2}{2}; \quad \tilde{V} = \frac{W_\chi^2}{2}. \quad (16)$$

These two different models may be connected via a specific function  $f$ , which is called deformation function. Such a link requires that  $\phi = f(\chi)$ , which leads us to

$$W_\phi(\phi) = W_\chi(\chi) f_\chi; \quad \phi_\chi = f_\chi = \left. \frac{W_\phi}{W_\chi} \right|_{\phi \rightarrow \chi}. \quad (17)$$

We can observe that the last equation is very similar to (12). Therefore, let us suppose that (17) can be rewritten as

$$\phi_\chi = \frac{W_\phi}{W_\chi} = \frac{a_1 W_\phi(\chi) + a_2 W_\phi(\phi, \chi) + a_3 W_\phi(\phi) + c_1 g(\chi) + c_2 g(\phi, \chi) + c_3 g(\phi)}{b_1 W_\chi(\chi) + b_2 W_\chi(\phi, \chi) + b_3 W_\chi(\phi)}, \quad (18)$$

where  $W_\phi(\chi)$ ,  $W_\phi(\phi, \chi)$ , and  $W_\phi(\phi)$  are equivalent since they are constructed with the deformation function  $f(\chi)$  and with its inverse. The analogous procedure is taken for the different forms of  $W_\chi$  and for the extra function  $g$ . Such a methodology corresponds the simplest path to combine fields  $\phi$  and  $\chi$ , and was successfully applied in cosmological scenarios [8, 9], and in the description of crystalline polyethylene molecule [10].

This last function is used to connect fields  $\phi$  and  $\chi$  in the effective two scalar field model. Moreover, the complete equivalence of the previous equation with (17) imposes the constraints  $a_1 + a_2 + a_3 = 1$ ,  $b_1 + b_2 + b_3 = 1$ , and  $c_1 + c_2 + c_3 = 0$ .

Consequently, once Eq. (18) has the same structure of Eq. (12), we are allowed to identify

$$W_\phi = a_1 W_\phi(\chi) + a_2 W_\phi(\phi, \chi) + a_3 W_\phi(\phi) + c_1 g(\chi) + c_2 g(\phi, \chi) + c_3 g(\phi); \quad (19)$$

$$W_\chi = b_1 W_\chi(\chi) + b_2 W_\chi(\phi, \chi) + b_3 W_\chi(\phi), \quad (20)$$

where  $W_\phi$  and  $W_\chi$  must satisfy the property

$$W_{\chi\phi} = W_{\phi\chi}, \quad (21)$$

leading us to a constraint for the function  $g$ , given by

$$b_2 W_{\chi\phi}(\phi, \chi) + b_3 W_{\chi\phi}(\phi) = a_1 W_{\phi\chi}(\chi) + a_2 W_{\phi\chi}(\phi, \chi) + c_1 g_\chi(\chi) + c_2 g_\chi(\phi, \chi). \quad (22)$$

So, in order to have an unique form of  $g$ , we must choose either  $c_1$  or  $c_2$  equals to zero. Another interesting feature about this extension method is that the analytical solutions of the deformed one field systems are going to automatically satisfy the equations of motion related to the effective two scalar field model.

#### IV. APPLICATION TO BRANEWORLD SCENARIOS

##### A. Example I - $\phi^4$ versus $\chi^6$

Let us firstly apply the extension method by considering the first-order differential equation

$$\phi' = \frac{1}{2} W_\phi(\phi) = a^2 - (\phi - a)^2, \quad (23)$$

whose analytical solution is

$$\phi(y) = a + a \tanh(ay). \quad (24)$$

Now, if we work with the deformation function

$$\phi = f(\chi) = 2a - \frac{a}{b^2} \chi^2, \quad (25)$$

we directly obtain the first-order differential equation

$$\chi' = \frac{1}{2} W_\chi(\chi) = -\frac{a}{2} \chi \left( 2 - \frac{\chi^2}{b^2} \right), \quad (26)$$

and the last one has solution given by

$$\chi(y) = b \sqrt{1 - \tanh(ay)}. \quad (27)$$

Therefore, we are able to use  $f$  and its inverse to write the relations

$$\frac{1}{2} W_\phi(\phi) = a^2 - (\phi - a)^2; \quad \frac{1}{2} W_\phi(\chi) = \frac{a^2}{b^2} \left( 2\chi^2 - \frac{\chi^4}{b^2} \right); \quad \frac{1}{2} W_\phi(\phi, \chi) = \frac{a^2}{b^2} \chi^2 \left( \frac{\chi^2}{b^2} + 2 \frac{\phi - a}{a} \right) \quad (28)$$

$$\frac{1}{2} W_\chi(\chi) = -\frac{a}{2} \chi \left( 2 - \frac{\chi^2}{b^2} \right); \quad \frac{1}{2} W_\chi(\phi, \chi) = -\frac{a}{2} \chi \left( 1 + \frac{\phi - a}{a} \right), \quad (29)$$

where we are not considering the form  $W_\chi(\phi)$  since we would like to avoid terms involving rational powers in the final form of our potential. Such a consideration is equivalent to take  $b_3 = 0$  in the extension method. Moreover, the constraint (22) with  $c_1 = 0$  yields to

$$\frac{c_2}{2} g(\phi, \chi) = -\frac{b_2}{4} \chi^2 - a_2 \frac{a^2}{b^2} \chi^2 \left( \frac{\chi^2}{b^2} + 2 \frac{\phi - a}{a} \right) - a_1 \frac{a^2}{b^2} \left( 2\chi^2 - \frac{\chi^4}{b^2} \right), \quad (30)$$

and we can use  $\chi = f^{-1}(\phi)$  to rewrite this last equation as

$$\frac{c_2}{2} g(\phi) = -b_2 \frac{b^2}{4} \left( 1 - \frac{\phi - a}{a} \right) - a^2 (a_1 + a_2) \left( 1 - \frac{(\phi - a)^2}{a^2} \right). \quad (31)$$

By putting all these ingredients into (19) and (20), we find

$$W(\phi, \chi) = -(1 - b_2) a \left( \chi^2 - \frac{\chi^4}{4b^2} \right) - \frac{b_2}{2} \phi \chi^2 + \frac{b_2 b^2}{2} \left( 2\phi - \frac{\phi^2}{2a} \right) + 2 \left( a\phi^2 - \frac{\phi^3}{3} \right), \quad (32)$$

and it is interesting to observe that if we choose  $b = \pm\sqrt{2}$ ,  $a = \pm 1/2$  e  $b_2 = 1$ ,  $W$  has the form

$$\frac{W}{2} = -\frac{1}{4} \phi \chi^2 + \phi - \frac{\phi^3}{3}, \quad (33)$$

which is the well known BNRT model for  $r = 1/4$  [11]. Now, let us go back to Eq. (9), where we can substitute  $W(\phi, \chi)$  together with the analytical solutions presented in (24) and (27), to determine that

$$A(y) = \frac{1}{36} \left[ -2ay (8a^2 + 3b^2(2b_2 - 1)) - 2 (8a^2 + 3b^2) \log [\cosh(ay)] + 4a^2 \operatorname{sech}^2(ay) + 3b^2 \tanh(ay) \right], \quad (34)$$

leading us to the warp-factors plotted in Fig. 1. Moreover, Fig. 2 depicts the explicit forms of the fields  $\phi$  and  $\chi$ . The panels of Fig. 1 unveil three different brane regimes, here called critical (dotted black curves), non-critical (dashed red curves), and supercritical (solid blue curves). The critical behavior of the brane can be determined by taking the following limits

$$\lim_{y \rightarrow \pm \infty} \frac{d}{dy} e^{2A(y)} = 0. \quad (35)$$

So, if we consider  $A(y)$  given by (34), we find the constraints

$$b_2 = 1; \quad b_2 = -\frac{8}{3} \frac{a^2}{b^2}, \quad (36)$$

where the last result unveils the critical behavior of the branes, as one can see in the left and in the right panels of Fig. 1, respectively. There we also realize that constant  $b_2$  controls the symmetry of the brane, and that the integrable branes can be found in the interval  $-\frac{8}{3} \frac{a^2}{b^2} < b_2 < 1$ . Out of such an interval, the brane enters in a supercritical regime, as it is shown in the thin blue curves of Fig. 1.

Withal, the energy density for such a model is

$$\begin{aligned} \rho(y) = & \left\{ \frac{1}{2} a^4 \text{sech}^4(ay) - \frac{1}{432} a^2 (6(4a^2 + b^2) \tanh(ay) - 8a^2 \tanh^3(ay) + 16a^2 + 3b^2 \tanh^2(ay) + 3b^2(4b_2 - 3))^2 \right. \\ & \left. + \frac{1}{8} \left( \frac{1}{16} (\tanh(ay) - 1)^2 (8a^2 \tanh(ay) + 8a^2 + b^2 b_2)^2 + a^2 b^2 (\tanh(ay) + 1) \text{sech}^2(ay) \right) + \frac{a^2 b^2 \text{sech}^4(ay)}{8(1 - \tanh(ay))} \right\} \\ & \times \exp \left[ \frac{1}{18} (-2ay(8a^2 + 3b^2(2b_2 - 1)) - 2(8a^2 + 3b^2) \log(\cosh(ay)) + 4a^2 \text{sech}^2(ay) + 3b^2 \tanh(ay)) \right], \quad (37) \end{aligned}$$

which is illustrated in details in Fig. 3. In such a figure we can observe that the analyzed branes have  $\rho$  asymptotic null, excluding the critical case, and the supercritical cases.

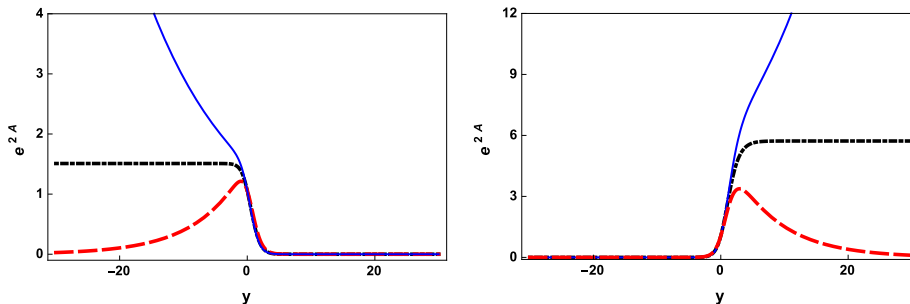


FIG. 1: In the left panel we see the warp-factor, for  $a = 1/2$ ,  $b = 2$ ,  $b_2 = 1$  (dotted black curve),  $b_2 = 0.9$  (dashed red curve), and  $b_2 = 1.05$  (solid blue curve), corresponding to critical, non-critical, and supercritical branes, respectively. In the right we worked with  $a = 1/2$ ,  $b = 2$ ,  $b_2 = -1/6$  (dotted black curve),  $b_2 = -1/6 + 0.1$  (dashed red curve), and  $b_2 = -1/6 - 0.05$  (solid blue curve).

### B. Example II - $p$ model versus $p$ model

In this example, we work with the first-order differential equation

$$\phi' = \frac{W_\phi}{2} = p \left[ \phi^{\frac{p-1}{p}} - \phi^{\frac{p+1}{p}} \right], \quad (38)$$

whose analytical solution is

$$\phi(x) = \tanh^p(y). \quad (39)$$

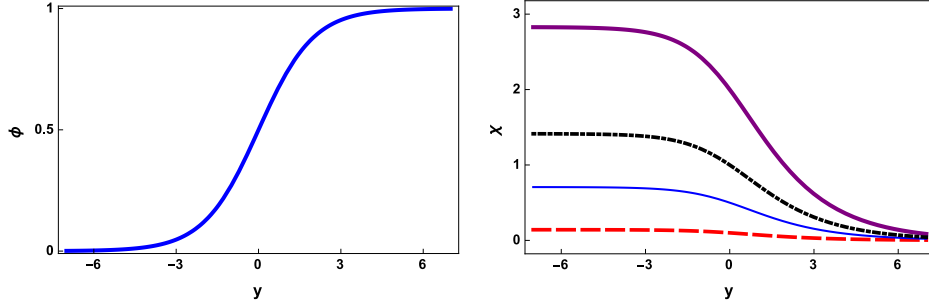


FIG. 2: The left panel shows  $\phi$  for  $a = 1/2$ . In the right frame we see  $\chi$  for  $a = 1/2$ ,  $b = 2$  (thicker violet curve),  $b = 0.1$  (dashed red curve),  $b = 0.5$  (solid blue curve) and  $b = 1.0$  (dotted dashed black curve).

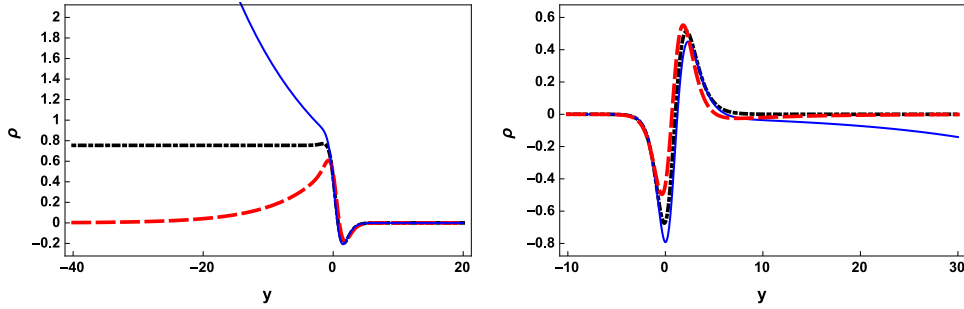


FIG. 3: In the left panel we see the energy density, for  $a = 1/2$ ,  $b = 2$ ,  $b_2 = 1$  (dotted black curve),  $b_2 = 0.9$  (dashed red curve), and  $b_2 = 1.05$  (solid blue curve). In the right we worked with  $a = 1/2$ ,  $b = 2$ ,  $b_2 = -1/6$  (dotted black curve),  $b_2 = -1/6 + 0.1$  (dashed red curve), and  $b_2 = -1/6 - 0.05$  (solid blue curve).

Then, by considering the simple deformation

$$\phi = \frac{\chi}{a}; \quad \chi = a \tanh^p(y), \quad (40)$$

we can rewrite (38) as

$$\chi' = \frac{W_\chi}{2} = ap \left[ \frac{\chi^{\frac{p-1}{p}}}{a} - \frac{\chi^{\frac{p+1}{p}}}{a} \right], \quad (41)$$

which is satisfied by the second equation of (40). So, repeating the methodology of the first example, we may rewrite  $W_\phi$  and  $W_\chi$  in the equivalent forms

$$\frac{W_\phi(\phi)}{2} = p(\phi^{\frac{p-1}{p}} - \phi^{\frac{p+1}{p}}), \quad \frac{W_\phi(\chi)}{2} = p \left[ \left( \frac{\chi}{a} \right)^{\frac{p-1}{p}} - \left( \frac{\chi}{a} \right)^{\frac{p+1}{p}} \right], \quad \frac{W_\phi(\phi, \chi)}{2} = p \left[ \left( \frac{\chi}{a} \right)^{\frac{p-1}{p}} - \phi \left( \frac{\chi}{a} \right)^{\frac{1}{p}} \right], \quad (42)$$

and

$$\frac{W_\chi(\chi)}{2} = pa \left[ \left( \frac{\chi}{a} \right)^{\frac{p-1}{p}} - \left( \frac{\chi}{a} \right)^{\frac{p+1}{p}} \right], \quad \frac{W_\chi(\phi)}{2} = pa(\phi^{\frac{p-1}{p}} - \phi^{\frac{p+1}{p}}), \quad \frac{W_\chi(\phi, \chi)}{2} = pa \left[ \left( \frac{\chi}{a} \right)^{\frac{p-1}{p}} - \phi \left( \frac{\chi}{a} \right)^{\frac{1}{p}} \right]. \quad (43)$$

In order to avoid negative exponent in the potential we choose  $c_1 = 0$  and  $b_3 = 0$ , which means that  $c_3 = -c_2$  and  $b_1 + b_2 = 1$ . Therefore, the function  $g(\phi, \chi)$  for this case is

$$\frac{c_2}{2} g(\phi, \chi) = -b_2 \frac{p^2 a^2}{p+1} \left( \frac{\chi}{a} \right)^{\frac{p+1}{p}} - a_2 p \left[ \left( \frac{\chi}{a} \right)^{\frac{p-1}{p}} - \phi \left( \frac{\chi}{a} \right)^{\frac{1}{p}} \right] - a_1 p \left[ \left( \frac{\chi}{a} \right)^{\frac{p-1}{p}} - \left( \frac{\chi}{a} \right)^{\frac{p+1}{p}} \right]. \quad (44)$$

By using the inverse of the deformation function, we can rewrite the last expression as

$$\frac{c_2}{2} g(\phi) = -b_2 \frac{p^2 a^2}{p+1} \phi^{\frac{p+1}{p}} - (a_2 + a_1) p \left( \phi^{\frac{p-1}{p}} - \phi^{\frac{p+1}{p}} \right). \quad (45)$$

Then, the application of the extension method yields to the effective superpotential:

$$\begin{aligned} W(\phi, \chi) = & 2 b_1 p^2 a^2 \left[ \frac{1}{2p-1} \left( \frac{\chi}{a} \right)^{\frac{2p-1}{p}} - \frac{1}{2p+1} \left( \frac{\chi}{a} \right)^{\frac{2p+1}{p}} \right] + 2 b_2 p^3 \frac{a^2 \phi^{\frac{2p+1}{p}}}{(p+1)(2p+1)} \\ & + 2 b_2 p^2 a^2 \left[ \frac{1}{2p-1} \left( \frac{\chi}{a} \right)^{\frac{2p-1}{p}} - \frac{\phi}{p+1} \left( \frac{\chi}{a} \right)^{\frac{p+1}{p}} \right] + 2 p^2 \left[ \frac{\phi^{\frac{2p-1}{p}}}{2p-1} - \frac{\phi^{\frac{2p+1}{p}}}{2p+1} \right] - 3 \tilde{c}, \end{aligned} \quad (46)$$

where  $\tilde{c}$  is an arbitrary real integration constant. Now, we can substitute this result together with the analytical solutions for  $\phi$  and  $\chi$  into (9) to determine that

$$A' = \frac{2 [p^2 (a^2 b_2 + 1) + 1] \left[ (2p-1) (\tanh(y))^{2p+1} - (2p+1) (\tanh(y))^{2p-1} \right]}{3(4p^2 - 1)} + \tilde{c}, \quad (47)$$

and we present bellow the explicit forms of  $A(y)$  for  $p = 1, 2, 3$  and  $4$ , together with their respective energy densities:

$$A_1 = -\frac{1}{9} (a^2 b_2 + 2) [4 \log(\cosh(y)) - \operatorname{sech}^2(y)] + \tilde{c} y; \quad (48)$$

$$A_2 = -\frac{1}{90} (4a^2 b_2 + 5) [3\operatorname{sech}^4(y) - 2\operatorname{sech}^2(y) + 8 \log(\cosh(y))] + \tilde{c} y; \quad (49)$$

$$A_3 = -\frac{1}{315} (9a^2 b_2 + 10) [-5\operatorname{sech}^6(y) + 12\operatorname{sech}^4(y) - 3\operatorname{sech}^2(y) + 12 \log(\cosh(y))] + \tilde{c} y; \quad (50)$$

$$A_4 = -\frac{1}{18144} (16a^2 b_2 + 17) \operatorname{sech}^8(y) [11 \cosh(2y) + 72 \cosh(4y) - 3 \cosh(6y) + 384 \cosh^8(y) \log(\cosh(y)) + 104] + \tilde{c} y; \quad (51)$$

$$\begin{aligned} \rho_1 = & \frac{1}{54} \left( \frac{27(a^4(b_2^2 + 1) + 2a^2(b_2 + 1) + 1) \operatorname{sech}^4(y)}{a^2} - 2(2(a^2 b_2 + 2) \tanh(y) (\tanh^2(y) - 3) + 9 \tilde{c})^2 \right) \\ & \times \exp \left( 2 \tilde{c} y - \frac{2}{9} (a^2 b_2 + 2) (4 \log(\cosh(y)) - \operatorname{sech}^2(y)) \right); \end{aligned} \quad (52)$$

$$\begin{aligned} \rho_2 = & \left( \frac{(8a^2(2a^2(b_2^2 + 1) + b_2 + 4) + 1) \tanh^2(y) \operatorname{sech}^4(y)}{8a^2} - \frac{1}{675} (2(4a^2 b_2 + 5) (3 \tanh^2(y) - 5) \tanh^3(y) + 45 \tilde{c})^2 \right) \\ & \times \exp \left( 2 \tilde{c} y - \frac{1}{45} (4a^2 b_2 + 5) (3\operatorname{sech}^4(y) - 2\operatorname{sech}^2(y) + 8 \log(\cosh(y))) \right); \end{aligned} \quad (53)$$

$$\begin{aligned} \rho_3 = & \left( \frac{(81a^4(b_2^2 + 1) + 18a^2(b_2 + 9) + 1) \tanh^4(y) \operatorname{sech}^4(y)}{18a^2} - \frac{(2(9a^2 b_2 + 10) (5 \tanh^2(y) - 7) \tanh^5(y) + 105 \tilde{c})^2}{3675} \right) \\ & \times \exp \left( 2 \tilde{c} y - \frac{2}{315} (9a^2 b_2 + 10) (-5\operatorname{sech}^6(y) + 12\operatorname{sech}^4(y) - 3\operatorname{sech}^2(y) + 12 \log(\cosh(y))) \right); \end{aligned} \quad (54)$$

$$\begin{aligned} \rho_4 = & \left( \frac{(32a^2(8a^2(b_2^2 + 1) + b_2 + 16) + 1) \tanh^6(y) \operatorname{sech}^4(y)}{32a^2} - \frac{(2(16a^2 b_2 + 17) (7 \tanh^2(y) - 9) \tanh^7(y) + 189 \tilde{c})^2}{11907} \right) \\ & \times \exp \left( 2 \tilde{c} y - \frac{(16a^2 b_2 + 17) \operatorname{sech}^8(y) (11 \cosh(2y) + 72 \cosh(4y) - 3 \cosh(6y) + 384 \cosh^8(y) \log(\cosh(y)) + 104)}{9072} \right) \end{aligned} \quad (55)$$

whose details can be appreciated in Figs. 4 and 5. There we see that when the integration constant  $\tilde{c} \neq 0$ , we have an asymmetric warp-factor. Again, we are able to use Eq. (35) to find the critical branes for each one of our warp-factors. By taking  $A_1$ , we derive that the constraints for critical branes are

$$\tilde{c} = \pm \frac{4}{9} (a^2 b_2 + 2), \quad (56)$$

therefore, we are able to compute integrable branes in the interval  $-\frac{4}{9} (a^2 b_2 + 2) < \tilde{c} < \frac{4}{9} (a^2 b_2 + 2)$ .

It is interesting to point that the warp-factor for  $A_4$  (dotted dashed violet curve), depicted in the left panel of Fig. 4, unveils a brane which is almost constant around  $y = 0$ , so, in such a region the brane is close to the four-dimensional Minkowski space-time, characterizing a bulk inside the fifth dimension. This behavior is corroborated by the energy density for this configuration (dotted dashed violet curve from Fig. 5), which is almost null around  $y = 0$ .

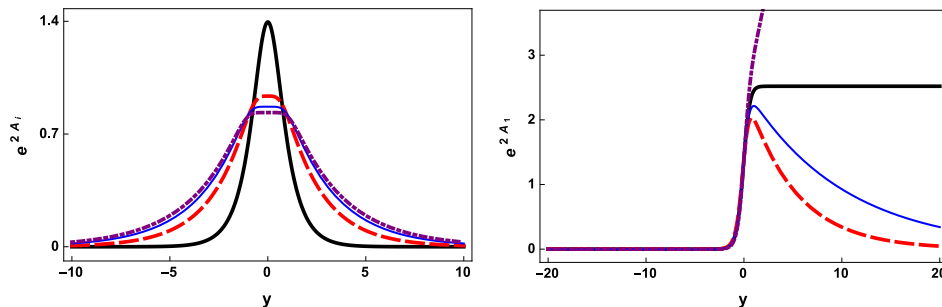


FIG. 4: In the left panel we see the warp-factors  $e^{2A_i}$ , with  $i = 1$  (solid black curve),  $i = 2$  (dashed red curve),  $i = 3$  (solid thin blue curve) and  $i = 4$  (dotted dashed violet curve), for  $a = 1$ ,  $b_2 = -0.5$ , and  $\tilde{c} = 0$ . In the right we plotted  $e^{2A_1}$  with  $a = 1$ ,  $b_2 = -0.5$ ,  $\tilde{c} = 2/3$  (solid black curve),  $\tilde{c} = 2/3 - 0.1$  (dashed red curve),  $\tilde{c} = 2/3 - 0.05$  (solid thin blue curve), and  $\tilde{c} = 2/3 + 0.1$  (dotted dashed violet curve).

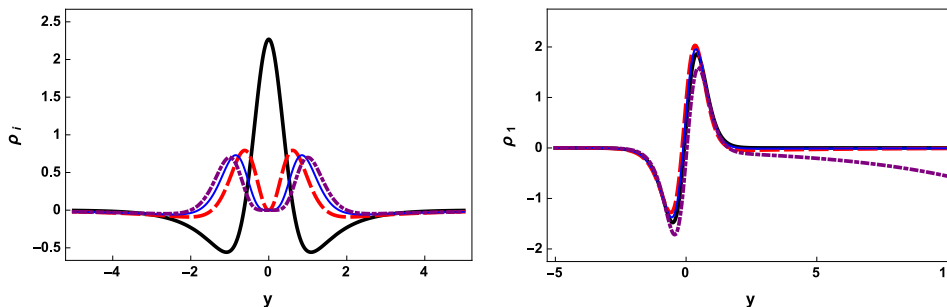


FIG. 5: The left frame shows the energy density  $\rho_i$ , with  $i = 1$  (solid black curve),  $i = 2$  (dashed red curve),  $i = 3$  (solid thin blue curve) and  $i = 4$  (dotted dashed violet curve), for  $a = 1$ ,  $b_2 = -0.5$ , and  $\tilde{c} = 0$ . In right frame we plotted  $\rho_1$  with  $a = 1$ ,  $b_2 = -0.5$ ,  $\tilde{c} = 2/3$  (solid black curve),  $\tilde{c} = 2/3 - 0.1$  (dashed red curve),  $\tilde{c} = 2/3 - 0.05$  (solid thin blue curve), and  $\tilde{c} = 2/3 + 0.1$  (dotted dashed violet curve).

### C. Example III - $\phi^4$ versus $p$ model

Another interesting analytical braneworld scenario raises from the coupling between the standard  $\phi^4$  with a  $p$  model. Here we consider the following kink-like profiles for the fields

$$\phi = \tanh(y); \quad \chi = a \tanh^p(y), \quad (57)$$



consequently, the deformation function which connects these two models is

$$\phi = \left(\frac{\chi}{a}\right)^{\frac{1}{p}}; \quad \chi = a \phi^p. \quad (58)$$

So, we have the following equivalent representations for  $W_\phi$  and  $W_\chi$ :

$$\frac{W_\phi(\phi)}{2} = 1 - \phi^2, \quad \frac{W_\phi(\chi)}{2} = 1 - \left(\frac{\chi}{a}\right)^{\frac{2}{p}}, \quad \frac{W_\phi(\phi, \chi)}{2} = \left(1 - \left(\frac{\chi}{a}\right)^{\frac{1}{p}}\right) (1 + \phi); \quad (59)$$

$$\frac{W_\chi(\chi)}{2} = p a \left( \left(\frac{\chi}{a}\right)^{\frac{p-1}{p}} - \left(\frac{\chi}{a}\right)^{\frac{p+1}{p}} \right), \quad \frac{W_\chi(\phi)}{2} = p a (\phi^{p-1} - \phi^{p+1}), \quad \frac{W_\chi(\phi, \chi)}{2} = p a \left( \left(\frac{\chi}{a}\right)^{\frac{p-1}{p}} - \phi^p \left(\frac{\chi}{a}\right)^{\frac{1}{p}} \right). \quad (60)$$

The last expressions enable us to obtain

$$\frac{c_2}{2} g(\phi, \chi) = b_3 p a [(p-1)\phi^{p-2} - (p+1)\phi^p] \chi - \frac{b_2 a^2 p^3}{p+1} \phi^{p-1} \left(\frac{\chi}{a}\right)^{\frac{p+1}{p}} - a_1 \left(1 - \left(\frac{\chi}{a}\right)^{\frac{2}{p}}\right) - a_2 \left(1 - \left(\frac{\chi}{a}\right)^{\frac{1}{p}}\right) (1 + \phi) \quad (61)$$

where we choose  $c_1 = 0$ . Moreover by using the inverse of the deformation function we directly determine

$$\frac{c_2}{2} g(\phi) = b_3 p a^2 [(p-1)\phi^{p-2} - (p+1)\phi^p] \phi^p - \frac{b_2 a^2 p^3}{p+1} \phi^{2p} - (a_1 + a_2) (1 - \phi^2). \quad (62)$$

These previous ingredients led us to the effective superpotential

$$\begin{aligned} W(\phi, \chi) &= 2 a^2 b_1 p^2 \left( \frac{\left(\frac{\chi}{a}\right)^{\frac{2p-1}{p}}}{2p-1} - \frac{\left(\frac{\chi}{a}\right)^{\frac{2p+1}{p}}}{2p+1} \right) + 2 \frac{a^2 b_2 p^3 \phi^{2p+1}}{(p+1)(2p+1)} + 2 \frac{a^2 b_2 p^2 \left(\frac{\chi}{a}\right)^{\frac{2p-1}{p}}}{2p-1} - 2 \frac{a^2 b_2 p^2 \phi^p \left(\frac{\chi}{a}\right)^{\frac{p+1}{p}}}{p+1} \\ &+ 2 a^2 b_3 p \left( \frac{(p+1)\phi^{2p+1}}{2p+1} - \frac{(p-1)\phi^{2p-1}}{2p-1} \right) + 2 a b_3 p \chi (\phi^{p-1} - \phi^{p+1}) - 2 \left( \frac{\phi^3}{3} - \phi \right) - 3 \tilde{c}, \end{aligned} \quad (63)$$

and by taking it back together with the static solutions to Eq. (9), we find

$$A' = -\frac{2}{9} \operatorname{sech}(y) \left( \frac{3a^2 p^2 \operatorname{csch}(y) (2p + \cosh(2y)) \tanh^{2p}(y)}{4p^2 - 1} + (\cosh(2y) + 2) \tanh(y) \operatorname{sech}(y) \right) + \tilde{c}, \quad (64)$$

therefore, the warp-factor and their respective energy densities for  $p = 1, 2, 3$  and  $4$  are given by

$$A_1 = \frac{1}{9} ((a^2 + 1) \operatorname{sech}^2(y) - 4(a^2 + 1) \log(\cosh(y))) + \tilde{c} y; \quad (65)$$

$$A_2 = \frac{1}{45} (-6a^2 \operatorname{sech}^4(y) + (4a^2 + 5) \operatorname{sech}^2(y) - 4(4a^2 + 5) \log(\cosh(y)) - 8a^2) + \tilde{c} y; \quad (66)$$

$$A_3 = \frac{1}{315} ((27a^2 + 35) \operatorname{sech}^2(y) - 4(27a^2 + 35) \log(\cosh(y)) - 9a^2(6 \cosh(2y) + 1) \operatorname{sech}^6(y) - 54a^2) + \tilde{c} y; \quad (67)$$

$$\begin{aligned} A_4 &= \frac{1}{567} \left( -3 ((64a^2 + 84) \log(\cosh(y)) + 32a^2) + (48a^2 + 63) \operatorname{sech}^2(y) \right. \\ &\quad \left. - a^2 (28 \cosh(2y) + 45 \cosh(4y) + 67) \operatorname{sech}^8(y) \right) + \tilde{c} y; \end{aligned} \quad (68)$$

$$\begin{aligned} \rho_1 &= \frac{1}{27} (\cosh(y))^{-\frac{8}{9}(a^2+1)} e^{\frac{2}{9}(a^2+1) \operatorname{sech}^2(y) + 2\tilde{c}y} \left( 72(a^2+1) \tilde{c} \tanh(y) + 36(a^2+1) \tilde{c} \tanh(y) \operatorname{sech}^2(y) \right. \\ &\quad \left. + 4(a^2+1)^2 \operatorname{sech}^6(y) + 3(a^2+1)(4a^2+13) \operatorname{sech}^4(y) - 16(a^2+1)^2 - 81\tilde{c}^2 \right); \end{aligned} \quad (69)$$

$$\rho_2 = \left( -\frac{1}{675} (24a^2 \tanh^5(y) + (10 - 40a^2) \tanh^3(y) + 45\tilde{c} - 30 \tanh(y))^2 - 2a^2 \text{sech}^6(y) + \text{sech}^4(y) (2a^2 \tanh^2(y) + 2a^2 + 1) \right) \exp \left( \frac{2}{45} (-6a^2 \text{sech}^4(y) + (4a^2 + 5) \text{sech}^2(y) - 4(4a^2 + 5) \log(\cosh(y)) - 8a^2 + 45\tilde{c}y) \right); \quad (70)$$

$$\rho_3 = \left( \text{sech}^4(y) (9a^2 \tanh^4(y) + 1) - \frac{(270a^2 \tanh^7(y) - 378a^2 \tanh^5(y) + 315\tilde{c} + 70 \tanh^3(y) - 210 \tanh(y))^2}{33075} \right) \quad (71)$$

$$\times \exp \left( 2 \left( \frac{1}{315} ((27a^2 + 35) \text{sech}^2(y) - 4(27a^2 + 35) \log(\cosh(y)) - 9a^2(6 \cosh(2y) + 1) \text{sech}^6(y) - 54a^2) + \tilde{c}y \right) \right);$$

$$\rho_4 = \frac{(\cosh(y))^{-\frac{8}{189}(16a^2+21)}}{11907} \left( (11907 \text{sech}^4(y) (16a^2 \tanh^6(y) + 1) \right. \quad (72)$$

$$\left. - (-32a^2(\cosh(2y) + 8) \tanh^7(y) \text{sech}^2(y) + 189\tilde{c} + 42 \tanh^3(y) - 126 \tanh(y))^2 \right)$$

$$\times \exp \left( -\frac{2}{567} (-3(16a^2 + 21) \text{sech}^2(y) + a^2(28 \cosh(2y) + 45 \cosh(4y) + 67) \text{sech}^8(y) + 96a^2 - 567\tilde{c}y) \right).$$

The previous relations are shown in the panels of Fig. 6 and 7, there we observe that asymmetric warp-factors appear if  $\tilde{c}$  is different of zero. Analogously to the previous examples, we can use the limits (35) to establish that the critical branes appear if

$$\tilde{c} = \pm \frac{4}{9} (a^2 + 1), \quad (73)$$

which means that integrable branes are constrained in the interval  $\frac{4}{9} (a^2 + 1) < \tilde{c} < \frac{4}{9} (a^2 + 1)$ .

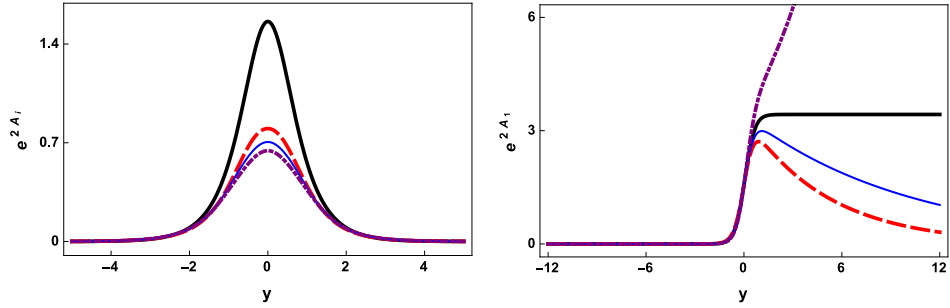


FIG. 6: In the left panel we see the warp-factors  $e^{2A_i}$ , with  $i = 1$  (solid black curve),  $i = 2$  (dashed red curve),  $i = 3$  (solid thin blue curve) and  $i = 4$  (dotted dashed violet curve), for  $a = 1$ , and  $\tilde{c} = 0$ . In the right we plotted  $e^{2A_1}$  with  $a = 1$ ,  $\tilde{c} = 8/9$  (solid black curve),  $\tilde{c} = 8/9 - 0.1$  (dashed red curve),  $\tilde{c} = 8/9 - 0.05$  (solid thin blue curve), and  $\tilde{c} = 8/9 + 0.1$  (dotted dashed violet curve).

## V. STABILITY OF THE BRANES

In order to discuss the stability of the gravitational sector for the braneworld scenarios, we are going to adopt the procedures used in ref. [4, 14]. So, by considering a metric perturbation given by

$$ds^2 = e^{2A(y)} (\eta_{\mu\nu} + \epsilon h_{\mu\nu}) dx^\mu dx^\nu - dy^2, \quad (74)$$

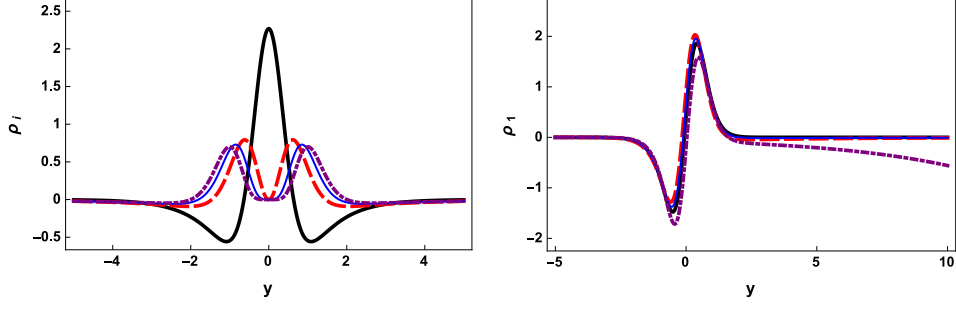


FIG. 7: The left frame shows the energy density  $\rho_i$ , with  $i = 1$  (solid black curve),  $i = 2$  (dashed red curve),  $i = 3$  (solid thin blue curve) and  $i = 4$  (dotted dashed violet curve), for  $a = 1$ , and  $\tilde{c} = 0$ . In right frame we plotted  $\rho_1$  with  $a = 1$ ,  $\tilde{c} = 8/9$  (solid black curve),  $\tilde{c} = 8/9 - 0.1$  (dashed red curve),  $\tilde{c} = 8/9 - 0.05$  (solid thin blue curve), and  $\tilde{c} = 8/9 + 0.1$  (dotted dashed violet curve).

where  $h_{\mu\nu}$  stands for the graviton with the axial gauge  $h_{5N} = 0$ , and if we take the metric fluctuation to be transverse and with null trace (which is denoted by  $\bar{h}_{\mu\nu}$ ), it is possible to prove that such fluctuation needs to satisfy the differential equation [4, 14]

$$\bar{h}''_{\mu\nu} + 4A'\bar{h}'_{\mu\nu} = e^{-2A}\square\bar{h}_{\mu\nu}. \quad (75)$$

Now, let us rescale the coordinate  $y$  by using the transformation  $dz = e^{-A(y)}dy$ , and let us also redefine  $\bar{h}_{\mu\nu}$  as

$$\bar{h}_{\mu\nu} = e^{ik \cdot x} e^{-\frac{3}{2}A(z)} H_{\mu\nu}, \quad (76)$$

such that the substitution of the previous definitions in the last differential equation results in

$$-\frac{d^2 H_{\mu\nu}}{dz^2} + U(z)H_{\mu\nu} = k^2 H_{\mu\nu}. \quad (77)$$

Therefore, we have a Schroedinger-like equation with effective potential

$$U(z) = \frac{3}{2}A_{zz} + \frac{9}{4}A_z^2. \quad (78)$$

The zero-mode ( $k = 0$ ) solution for (77) has the following general form

$$H_{\mu\nu}(z) = N_{\mu\nu} e^{\frac{3}{2}A(z)}, \quad (79)$$

where  $N_{\mu\nu}$  is a normalization constant. We can use the prerogative establish by [15], to set the equality

$$A_z = e^{A(y)} \frac{dA}{dy}; \quad A_{zz} = (A'' + A'^2) e^{2A(y)}, \quad (80)$$

which allows us to rewrite the Schroedinger-like potential as

$$U(y) = \frac{3}{4}e^{2A(y)} (2A'' + 5A'^2). \quad (81)$$

Moreover, in order to write the zero modes in terms of  $y$ , we can apply the change of variable  $\bar{h}_{\mu\nu} = e^{-2A(y)} \xi_{\mu\nu}(y) e^{ik \cdot x}$  in (75), yielding to

$$\frac{d^2 \xi_{\mu\nu}}{dy^2} - 4A'^2 \xi_{\mu\nu} - e^{-2A(y)} k^2 \xi_{\mu\nu} = 0, \quad (82)$$

then, the solution for the zero-mode has to obey the equation

$$\left( \frac{d}{dy} + 2A' \right) \left( \frac{d}{dy} - 2A' \right) \xi_{\mu\nu} = 0. \quad (83)$$

Consequently, the zero-mode eigenstate is such that

$$\xi_{\mu\nu} = N_{\mu\nu} e^{2A(y)}. \quad (84)$$

In Fig. 8, 9 and 10 we can see the effective confining potentials for examples I, II and III respectively, besides, some of them exhibit volcano shapes as shown in the left panels of Figs. 9, and 10. In Fig. 8, the dotted black curve corresponds to the effective confining potential related with a critical brane, while the dashed red curve stands for the case of a non-critical brane, and the blue solid curve describes the supercritical brane regime. Besides, in Figs. 9, and 10 we present the solid black curve as the effective potential for a critical brane, while the dashed red curve and the solid thin blue curve correspond to non-critical branes, and the dotted-dashed violet curve stands for the supercritical brane. As the reader can see, the graphics from Fig. 9, and 10 became more symmetric as we take  $\tilde{c}$  closer to zero. Those potentials which can localize gravity together with the zero-mode solutions, characterizes the stability of the branes (even for the asymmetric ones), except for the critical, and supercritical configurations, as expected.

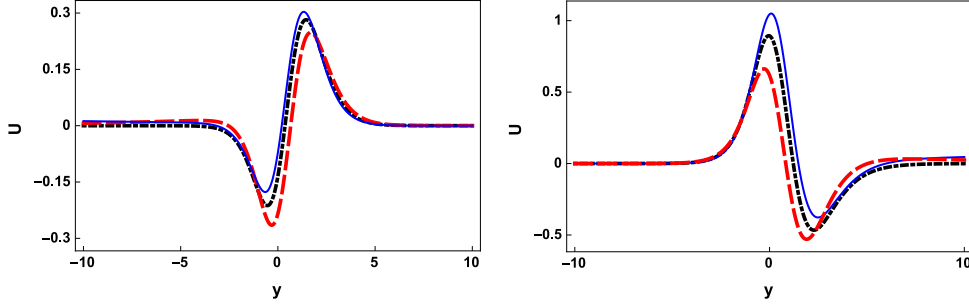


FIG. 8: In the left panel we see the effective potential, for  $a = 1/2$ ,  $b = 2$ ,  $b_2 = 1$  (dotted black curve),  $b_2 = 0.9$  (dashed red curve), and  $b_2 = 1.05$  (solid blue curve). In the right we worked with  $a = 1/2$ ,  $b = 2$ ,  $b_2 = -1/6$  (dotted black curve),  $b_2 = -1/6 + 0.1$  (dashed red curve), and  $b_2 = -1/6 - 0.05$  (solid blue curve).

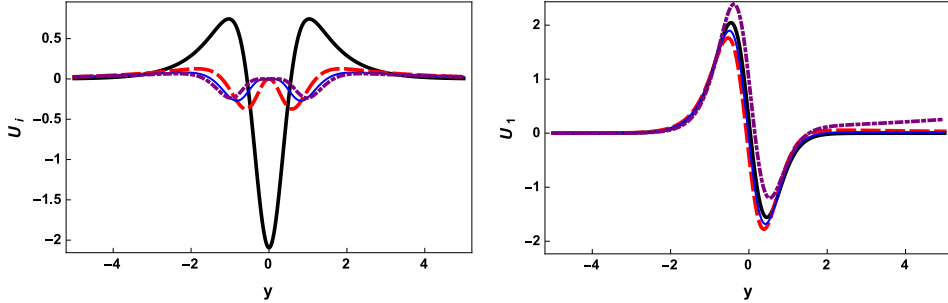


FIG. 9: In the left panel we see  $U_i$ , with  $i = 1$  (solid black curve),  $i = 2$  (dashed red curve),  $i = 3$  (solid thin blue curve) and  $i = 4$  (dotted dashed violet curve), for  $a = 1$ ,  $b_2 = -0.5$ , and  $\tilde{c} = 0$ . The right frame shows  $U_1$  with  $a = 1$ ,  $b_2 = -0.5$ ,  $\tilde{c} = 2/3$  (solid black curve),  $\tilde{c} = 2/3 - 0.1$  (dashed red curve),  $\tilde{c} = 2/3 - 0.05$  (solid thin blue curve), and  $\tilde{c} = 2/3 + 0.1$  (dotted dashed violet curve).

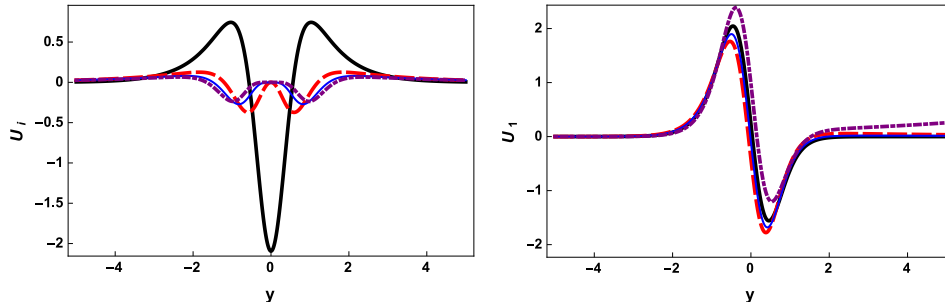


FIG. 10: In the left panel we see  $U_i$ , with  $i = 1$  (solid black curve),  $i = 2$  (dashed red curve),  $i = 3$  (solid thin blue curve) and  $i = 4$  (dotted dashed violet curve), for  $a = 1$ , and  $\tilde{c} = 0$ . The right frame shows  $U_1$  with  $a = 1$ ,  $\tilde{c} = 8/9$  (solid black curve),  $\tilde{c} = 8/9 - 0.1$  (dashed red curve),  $\tilde{c} = 8/9 + 0.1$  (dotted dashed violet curve).

## VI. DISCUSSIONS

In this work, we verified how the extension method can be successfully applied to hybrid braneworld scenarios. The methodology based on superpotential followed the steps of references [4, 7]. Such an application led us to construct more general two field braneworld models, besides it allowed us to recover some well-known results presented in [4]. Moreover, we could derive both symmetric and asymmetric branes for each one of the examples, besides the critical case. These regimes were predicted by imposing the asymptotic behavior for the derivative of the warp-factor shown in (35). The stability is normally associated with the existence of the zero mode, which guarantees the existence of four-dimensional gravity localized on the brane. The critical cases, however, do not enjoy the existence of normalizable zero modes, then, in principle, no four-dimensional gravity is localized on these branes. However, as shown in a series of papers [16–20], the asymmetric branes with no zero modes can localize four-dimensional gravity through massive gravity modes. This is known as metastable gravity, firstly reported in [21, 22]. We hope to bring in near future stability analysis from the perspective of such metastable scenarios. Moreover, the presented methodology generalizes the results derived from Bazeia and Gomes in [4] and can be applied to other braneworld investigations presented in the literature. We also believe that this procedure can be generalized to engender braneworlds composed of three or more fields.

## Acknowledgments

The authors would like to thank CAPES and CNPq (Brazilian agencies), for financial support during this work. FAB and JRLS acknowledge support from CNPq Grants no. 312104/2018-9 and 420479/2018-0, respectively.

- 
- [1] Lisa Randall, and R. Sundrum, Phys. Rev. Lett. **83**, 3370 (1999).
  - [2] Lisa Randall, and R. Sundrum, Phys. Rev. Lett. **83**, 4690 (1999).
  - [3] N. Arkani-Hamed, and M. Schmaltz, Phys. Rev. D **61**, 033005 (2000).
  - [4] D. Bazeia, and A. R. Gomes, JHEP **0405**, 012 (2004).
  - [5] A. de Souza Dutra, G. P. de Brito, and J. M. Hoff da Silva, Europhys. Lett. **108**, 11001 (2014).
  - [6] D. Bazeia, M. A. Marques, and R. Menezes, Phys. Rev. D **92**, 084058 (2015).
  - [7] D. Bazeia, L. Losano, and J.R.L. Santos, Physics Letters A **377**, 1615 (2013).
  - [8] P.H.R.S. Moraes, and J.R.L. Santos, Phys. Rev. D **89**, 083516 (2014).
  - [9] J.R.L. Santos, P.H.R.S. Moraes, D.A. Ferreira, and D. C. Vilar Neta, Eur. Phys. J. C **78**, 169 (2018).
  - [10] J.R.L. Santos, D.S.S. Borges, and I.O. Moreira, EPL **123**, 23001 (2018).
  - [11] D. Bazeia, J. R. S. Nascimento, R. F. Ribeiro, and D. Toledo, J. Phys. A: Math. Gen. **30** 8157 (1997).
  - [12] D. Bazeia, L. Losano, and J.M.C. Malbouisson, Phys. Review D **66**, 101701 (2002).
  - [13] D. Bazeia, and L. Losano, Phys. Rev. D **73**, 025016 (2006).
  - [14] W.T. Cruz, L.J.S. Sousa, and R.V. Maluf, C.A.S. Almeida, Phys. Lett. B **730** 314 (2014).

- [15] A. Campos, Phys. Rev. Lett. **88**, 141602 (2002).
- [16] R. C. Fonseca, F. A. Brito and L. Losano, arXiv:1611.03843 [hep-th].
- [17] R. C. Fonseca, F. A. Brito and L. Losano, Phys. Lett. B **728**, 443 (2014).
- [18] R. C. Fonseca, F. A. Brito and L. Losano, JCAP **1201**, 032 (2012).
- [19] R. C. Fonseca, F. A. Brito and L. Losano, Phys. Lett. B **697**, 493 (2011).
- [20] D. Bazeia, F. A. Brito and L. Losano, JHEP **0611**, 064 (2006).
- [21] G. R. Dvali, G. Gabadadze and M. Porrati, Phys. Lett. B **485**, 208 (2000).
- [22] R. Gregory, V. A. Rubakov and S. M. Sibiryakov, Phys. Rev. Lett. **84**, 5928 (2000).